듀티 제어가 적용된 3레벨 LLC 컨버터의 정상상태 및 소신호 모델링

후세인 휴마라, 김학원, 조관열
한국교통대학교

Steady State Analysis & Small Signal Modeling of Variable Duty Cycle Controlled Three Level LLC Converter

Hussain Humaira, Hag-Wone Kim, Kwan-Yuhl Cho
Korea National University of Transportation

ABSTRACT

In this paper, a three level duty cycle controlled half bridge LLC converter for EV charger application is presented. The topology and operating regions of the converter are discussed. The equations of the converter are derived in time domain. A small signal model of the converter is developed by perturbation and linearization of the steady state model about their operating point using Extended Describing function.

1. Introduction

LLC resonant converters are gaining popularity in industrial applications such as electrical vehicle chargers, renewable energy etc. due to its ability to achieve high efficiency at a wide input operation range while providing soft-switching. However, amount of research conducted on duty controlled LLC converter or three level LLC is very limited [1-3].

This paper introduces a half bridge three level LLC series resonant converter driven by duty controlled PWM signals. The small signal model is achieved by applying extended describing functions for duty controlled output.

2. Three Level LLC Converter

2.1 Circuit topology

The circuit configuration of the three level LLC converter is presented in Fig, 1. The circuit contains 4 MOSFET switches S1~S4 in half bridge configuration. The switches S1 and S4 are driven by duty controlled signals (D <=0.5).

1.2 Circuit operations

The proposed LLC converter operates in six modes.

The operating waveforms are shown in Fig. 2. The operation
modes and the steady state operation are discussed below in time domain:

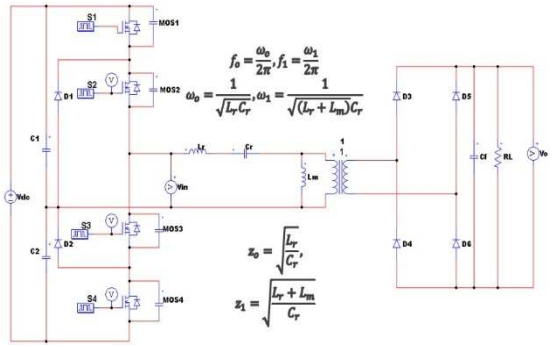

Fig.1 Schematic of three level LLC series resonant converter

1. Mode 1 $(t_0-t_1)=T_1$:
   This interval starts when S1 & S4 is turned on. I_{Lm} and I_{Lr} starts to increase.

2. Mode 2 $(t_1-t_2)=T_2$:
   This interval begins when S1 is turned off and S4 is on. I_{Lm} is still increasing but I_{Lr} starts to decrease.

3. Mode 3 $(t_2-t_3)=T_3$:
   When I_{Lr} becomes equal to I_{Lm}, mode 3 begins.

The modes t_3-t_4, t_4-t_5 and t_5-t_6 are similar to the first half of the operational modes but opposite in polarity. The difference between I_{Lr} and I_{Lm} i.e energy from t_0 to t_2 is transferred to the secondary. The output is clamped at L_m. The operational waveforms are given in Fig. 2 and the describing equations are summarized in Fig. 3. Unlike two level LLC resonant converters [4], the time intervals and initial conditions are rather complex to analyze. This paper aims to approximate the initial conditions and time interval under certain load conditions.

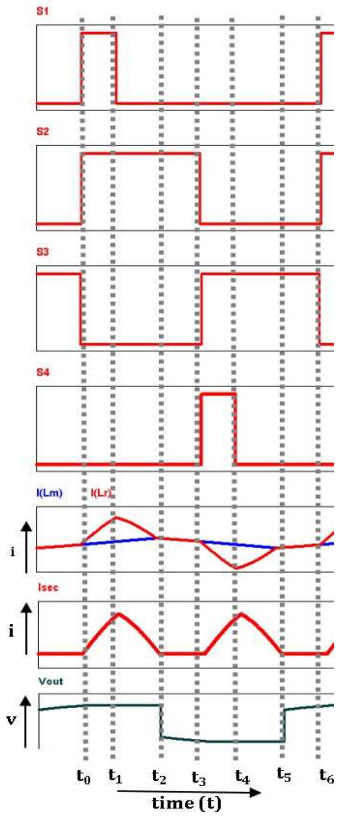

Fig.2 Operational waveforms of three level LLC series resonant converter

Mode 1 $(t_0-t_1)=T_1$	Mode 3 $(t_2-t_3)=T_3$
$I_{Lr}(T_1)=\frac{1}{z_{in}}(V_{in}-V_o-V_{cro})sin\omega_o T_1+I_{Lro}\cos\omega_o T_1$ (1) $I_{Lm}(T_1)=\left(\frac{V_o T_1}{L_{in}}\right)+I_{Lmo}$ (2) $V_{Cr}(T_1)=(V_{in}-V_o)+z_o I_{Lro}\sin\omega_o T-(V_T-V_o-V_{cro})\cos\omega_o T_1$ (3)	$I_{Lr}(T_3)=\frac{1}{z_1}(-V_o-V_{cr1})sin\omega_1 T_1+I_{Lr1}\cos\omega_1 T_2$ (7) $I_{Lm}(T_2)=\left(\frac{V_o T_2}{L_m}\right)+I_{Lm1}$ (8) $V_{Cr}(T_2)=(-V_o)+(V_o+V_{cro})\cos\omega_1 T_2$ (9)
Mode 2 $(t_1-t_2)=T_2$:	Power Transfer stage
$I_{Lr}(T_2)=\frac{1}{z_1}(-V_o-V_{cr1})sin\omega_1 T_1+I_{Lr1}\cos\omega_1 T_2$ (4) $I_{Lm}(T_2)=\left(\frac{V_o T_2}{L_m}\right)+I_{Lm1}$ (5) $V_{Cr}(T_2)=(-V_o)+(V_o+V_{cro})\cos\omega_1 T_2$ (6)	$I_o=\frac{\int_{t_0}^{t_2}(I_{Lr}(t)-I_{Lm}(t)}{\frac{T_s}{2}}$ (10) $=\frac{2}{T_s}\left[\left\{\frac{1}{z_o\omega_o}(V_{in}-V_o-V_{cro})(1-\cos\omega_o T_1)+\frac{1}{\omega_o}I_{Lro}\sin\omega_o T_1-\frac{V_o}{2Lm}T_1^2\right\}+\left\{\frac{1}{z_1\omega_1}(V_o-V_{cr1})(1-\cos\omega_1 T_2)+\frac{1}{\omega_o}I_{Lr1}\sin\omega_1 T_2-\frac{V_o}{2Lm}T_2^2\right\}\right]$ (11)

Fig.3 The state space equations of 3-level LLC Converter.

The time t1 can be described as $t_1=\frac{DT_s}{2}$, where T_s =switching period However solving for the time T_2 is further complex and has scope for research. This paper uses a linear regression model using the simulation data:

$T_2=\frac{f_o}{3}(1-D)-\frac{C_r}{5.55}R_L$ (12)

So the interval T_3 is equal to $T_3=1-T_1-T_2$. The initial conditions of current and voltage are approximated by the following:

$I_{Lm}(t_2)=I_{Lr}(t_2)=I_{Lmpeak}=\frac{V_o}{4L_m f_o}$ (13)

$I_{Lm}(t_0)=I_{Lr}(t_0)=-I_{Lr}(t_3)=-I_{Lm}(t_3)\approx 0.5\times I_{Lmpeak}$ (14)

$$\left.\begin{array}{l} V_{cro}=-V_{dc}\times D, D\le 0.2, \\ V_{cro}=-V_{dc}\times(D-0.05), \\ 0.2<D<0.5, \\ V_{cro}=-V_{dc}\times(D-0.1), D=0.5 \end{array}\right\} \quad (15)$$

The initial value approximation has been conducted for high load condition. The values are approximately similar and thus load parameter has not been included. The above equations can be verified through simulation.

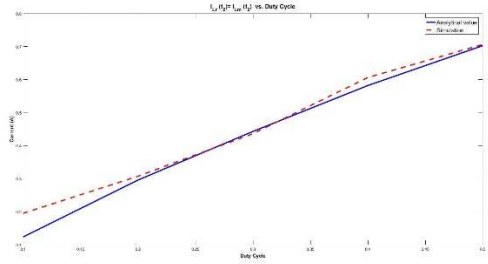

(a)

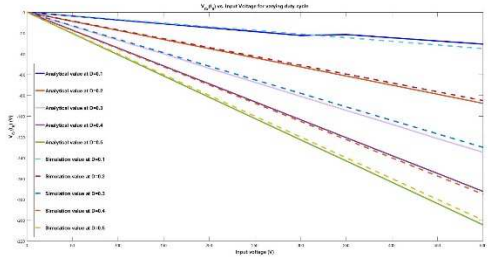

(b)

Fig.4 Initial values of (a) $I_{Lm}(t_2)=I_{Lr}(t_2)$ (b) V_{cro}

3. Small Signal Equivalent Circuit model

The large signal model is achieved through E. Yang's method [5,6]. Consequently, the model and perturbed and linearized around the operating point to obtain the small signal model. The state variables and the input variables are expressed as: $x=\left[\hat{\imath}_{Lrs}\ \hat{\imath}_{Lrc}\ \hat{\imath}_{Lms}\ \hat{\imath}_{Lmc}\ \hat{v}_{Crs}\ \hat{v}_{crc}\ \hat{v}_{cf}\right]^T$ and $u=[\hat{d}\ \hat{\omega}_s]^T$, where $\hat{d}$ and $\hat{\omega}_s$ is the perturbed value of duty and frequency. The converter is operated at resonant frequency when duty control is performed. Upon deriving control-output transfer function, the model can be verified and the controller can be designed. The small signal model is presented in Fig.5 and bode plot is given in Fig. 6 according to Eq. (16) and simulation via MATLAB.

$$\frac{\hat{v}_o}{\hat{d}}=\frac{s\left\{k_s V_g\cos(\frac{\pi}{2}D)R_L C_f\right\}+k_s V_g\cos(\frac{\pi}{2}D)R_L C_f}{s^2 L_e C_f-s\left(2k^2{}_s\sin(\frac{\pi}{2}D)R_L C_f-rC_f\right)-2k^2{}_s\sin(\frac{\pi}{2}D)} \quad (16)$$

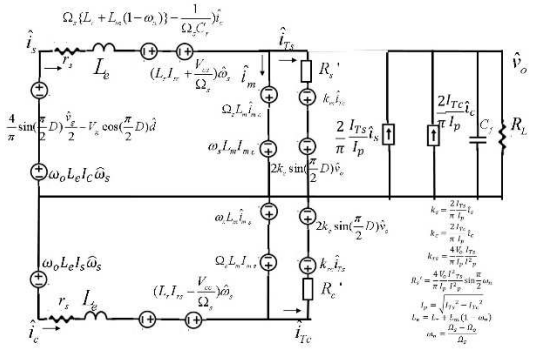

Fig.5 Small signal model of the proposed converter

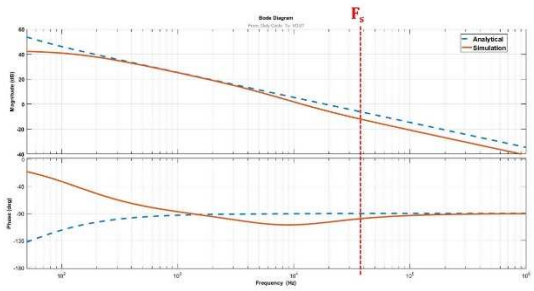

Fig.6 Bode Plot of control-output transfer function.

The parameters of the simulated converter are as follows: V_g=100V, Lr= 41.2 μH, C_r=500nF, F_s=35.5 KHz, C_f = 220 μH, R_L=15Ω. When operated at resonant frequency, for duty controlled output, the control to output transfer function is reduced to second order. The transfer functions are much simpler to derive in case of duty control. A voltage controlled compensator can be designed from the bode plot.

This research was supported by a grant(19RTRP-B146008-02) from Railroad Technology Research Program funded by Ministry of Land, Infrastructure and Transport of Korean Government.

4. Conclusion

The three level LLC converter has been analyzed and modeled and can be regulated by duty cycle. The control-output transfer function is of reduced order due to duty control method. The analysis can be further verified through simulation.

참 고 문 헌

[1] B. Yang, F.C. Lee, A.J. Zhang and G. Huang, "LLC Resonant Converter For Front End DC-DC Conversion," in Proc. IEEE APEC, 2002, vol. 2, pp. 1108-1112.

[2] I.O Lee, G.W Moon, "Analysis and Design of a Three Level LLC series Resonant Converter for High and Wide Input Voltage Applications", in IEEE Transactions on Power Electronics, Vol. 27, No. 6, pp. 2966-2979, 2012, June.

[3] G. Cai, D. Liu,C. Liu,W. Li, Jiajun Sun "A High-Frequency Isolation (HFI) Charging DC Port Combining a Front-End Three-Level Converter with a Back-End LLC Resonant Converter," in Energies, Vol. 10, No. 10, pp. 1462, 2017, September.

[4] N. Shafiei, M. A. Saket and M. Ordonez, "Time domain analysis of LLC resonant converters in the boost mode for battery charger applications," 2017 IEEE Energy Conversion Congress and Exposition (ECCE), pp. 4157-4162, 2017.

[5] C S. Tian, F. C. Lee and Q. Li, "A Simplified Equivalent Circuit Model of Series Resonant Converter," in IEEE Transactions on Power Electronics, Vol. 31, No. 5, pp. 3922-3931, 2016, May.

[6] Y.J Choi, H.R Cha, S.M Jungm R.Y Kim, "An Integrated Current-Voltage Compensator Design Method for Stable Constant Voltage and Current Source Operation of LLC Resonant Converters" in Energies, Vol. 11, No. 6, pp. 1325, 2018, May.